Biophysical Chemistry, 49 (1994) 91–99
Elsevier Science B.V., Amsterdam

BIOCHE 1832

Proton diffusion on purple membrane studied by neutron scattering

R.E. Lechner, N.A. Dencher [1]
Hahn-Meitner-Institut, Glienicker Strasse 100, D-14109 Berlin (Germany)

J. Fitter, G. Büldt
Freie Universität, FB Physik, Arnimallee 14, D-14195 Berlin (Germany)

and

A.V. Belushkin [2]
Rutherford Appleton Laboratory, Chilton, Oxon, OX110QX (UK)

(Received 10 July 1993; accepted in revised form 4 October 1993)

Abstract

Oriented stacks of purple membrane (PM) were studied with high-resolution quasielastic incoherent neutron scattering (QINS). The experiments were carried out under dark conditions at room temperature, for two different orientations, such that the momentum transfer Q was either parallel or perpendicular to the membrane plane at 90° scattering angle. The samples were equilibrated in H_2O as well as in D_2O, both at 100% relative humidity. The analysis of the spectra shows that the hydration water is performing anisotropic translational diffusion (TD), preferentially parallel to the membrane plane, with a diffusion coefficient about 5 times smaller than that of bulk water at room temperature. From the behaviour at large scattering angles an average jump distance of about 4 Å was estimated. This fast translational diffusion process is accompanied by an even faster local diffusive motion of the water protons. The approximate description of the latter by a rotational diffusion model for H_2O molecules yields a quasielastic line width of about 70 μeV (HWHM). The observed local diffusive motion of protons in PM is an order of magnitude slower (angular average of the corresponding linewidth: HWHM = 9 μeV).

Keywords: Neutron scattering; Purple membrane; Proton diffusion

1. Introduction

Purple membrane (PM) is formed from bacteriorhodopsin (BR) trimers in a well-ordered two-

[1] Present address: Inst. f. Biochemie, TH Darmstadt, Petersenstrasse 22, D-64287 Darmstadt, Germany.
[2] Permanent address: Frank Lab. of Neutron Physics, JINR, Dubna, Russian Federation.

SSDI 0301-4622(93)E0086-K

dimensional hexagonal lattice, which is embedded in a lipid bilayer matrix [1–3]. Each BR molecule is a proton pump used by *Halobacterium halobium* to convert sun light into electrochemical energy by the generation of a proton gradient across the membrane [4,5]. Very little is known about the dynamics of the corresponding proton translocation mechanism. For instance, one would like to know the H^+ pathways [6] on and through the membrane and the time scales corresponding to the different stages of the related proton motion, as well as the role of water molecules as vehicles for proton transfer, and in particular as mediators between different protonable sites of PM, and especially of BR.

In principle, the proton is *itself* an excellent probe for the study of its own motion as an individual ion or as a part of larger units such as OH^-, H_2O, H_3O^+, or any other molecule containing hydrogen atoms, including H-bonded networks. Due to its large cross section it dominates the intensity in quasielastic incoherent neutron scattering (QINS) experiments, which are suitable for investigating proton motions in the time range from 10^{-12} to 10^{-8} s. The obvious difficulty in studying specifically the proton pumping mechanism with QINS is the fact that only a very small number of protons are directly participating in this process, while all the hydrogen nuclei of the membrane are contributing to the scattered intensity. On the other hand, it should for the same reasons be much easier to study the dynamics of water molecules in the membrane's hydration layer, which represents a sizeable weight fraction of the whole system. At any rate, it is necessary to obtain comprehensive information on the dynamics of all the protons in PM, before one can hope to isolate the presumably rather small effects of proton motion, directly related to photoactivity. With this in mind we have started QINS experiments on PM in 1991. The first experiments were carried out with the time-of-flight spectrometer IN5 at ILL, Grenoble, using an elastic energy resolution of about 63 μeV (FWHM). The samples, studied under dark conditions, consisted of oriented PM stacks with two different degrees of hydration, defined by equilibration at relative humidities (r.h.) of 86% and 100%, respectively. A phenomenological analysis of the observed QINS spectra, carried out with the aim of separating contributions from different molecular subunits, gave the following essential results [7]:

At low hydration (86% r.h.) only local diffusive proton motions were observed at the given energy resolution. In particular, the water molecules appear to perform a preferential local diffusive motion parallel to the membrane plane. At 100% r.h. there is a strong indication of long-range translational diffusion (TD) involving water protons, although other explanations such as a combination of several different local diffusive proton motions would also be consistent with the data. For the TD model the estimation of the self-diffusion coefficient, D_s, gave a value of 8×10^{-6} cm^2/s, which is about three times smaller than that of bulk water at 300 K.

In order to reach a more decisive conclusion, we have carried out further measurements at higher energy resolution, as a function of membrane plane orientation, using the same kind of samples hydrated at 100% r.h., alternatively with H_2O and D_2O. In the present paper we analyze the spectra from these H_2O and D_2O containing PM specimens, with the aim of elucidating the specific dynamics of the hydration water. In this context the contribution of PM (including that of the BR molecules) to the scattering will be treated phenomenologically. An attempt to interpret this in a biophysically relevant manner will be discussed in a later publication.

2. The QINS experiment

The experiment was carried out using the inverted time-of-flight spectrometer IRIS [8] at the Rutherford–Appleton Laboratory, with pyrolytic graphite (PG) and mica crystals as analyzers. Only the PG results, obtained with an analyzer wavelength of $\lambda = 6.6518$ Å and an elastic energy resolution of about 16 μeV (FWHM), in an energy window from −400 to 400 μeV, will be discussed here. The spectra were taken at room temperature under dark conditions at 51 different scattering angles in the range $20° < \phi < 160.8°$. They were added together within 11 angular

groups, in order to improve the statistics and to reduce computer time. Two different sample orientations α were studied, so that for the scattering angle $\phi = 90°$ the elastic Q vector was perpendicular ($\alpha = 45°$) and parallel ($\alpha = 135°$) to the membrane plane, respectively (fig. 1). The PM stacks had been oriented by drying at 86% r.h. on aluminium foils, followed by equilibration at 100% r.h. and subsequently sealed in circular slab-shaped aluminium containers (sample diameter 50 mm). The amount of sample material used (including water) was 962 mg PM(H_2O) and 956 mg PM(D_2O), with transmission values of $T(90°) = 0.704$ and 0.746, respectively. Each sample contained 750 mg PM as determined by weighing the samples dried in vacuum after the end of the experiment. Vanadium standard and empty container spectra were measured with identical geometry.

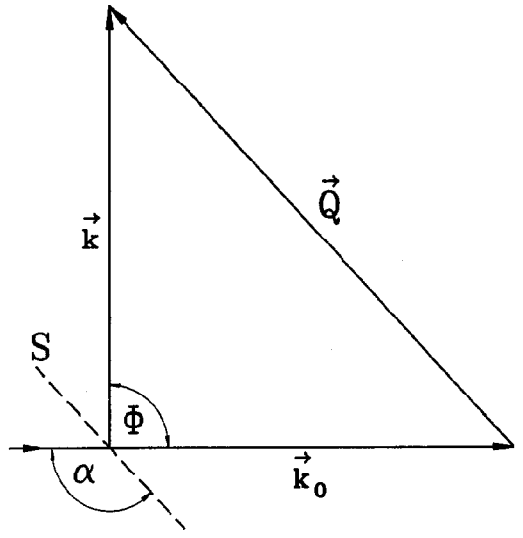

Fig. 1. Wavevector diagram of QINS experiment showing the relationship, $Q = k - k_0$, between incident (k_0) and scattered (k) neutron wavevectors, scattering vector Q, scattering angle ϕ and sample angle α, for the case $\phi = 90°$ and $\alpha = 135°$. The orientation of the membrane planes is indicated by a dashed line.

3. Method of comparing PM(H_2O) and PM(D_2O) spectra

In order to analyze the scattering of the hydration layer in the presence of the total scattering (of PM plus H_2O) we have applied the following method: at first a purely phenomenological expression for the scattering function was found, which perfectly fits the PM(D_2O) spectra. Then a model for H_2O was added to this expression and this was fitted to the PM(H_2O) spectra, in order to determine dynamical parameters of the hydration water. This method implies the following simplifications:

(i) The spectra of PM(H_2O) (and analogously those of PM(D_2O)) are approximated as arithmetic sums of intensities scattered by PM and by the hydration water, respectively. This is certainly true for first-order incoherent scattering, which represents about 75% of the total intensity. The remaining 25% are however due to multiple scattering (MSC) events comprising H_2O–H_2O and H_2O–PM combinations. Thus the MSC part of the hydration water spectra is directly affected by the presence of PM as a scatterer. This has not been taken into account explicitly in our calculations, since at this stage of the analysis MSC has been neglected altogether. Note however the following: Although the MSC contribution to the scattering is indeed of the order of 25%, we do not expect an error of more than about 10% on incoherent structure factors and QINS linewidths determined in the analysis of the total scattered intensity, which will be described below (sections 4 and 5). This order of magnitude is governed by the value of the sample transmission and is known from many previous MSC calculations carried out in connection with the analysis of other experiments; see, for instance ref. [9]. We will return to this question in the discussion (see section 6).

(ii) The scattering of D_2O is not considered separately; it is contained implicitly in the phenomenological expression found for PM(D_2O). Representing the scattering of PM(H_2O) by that of PM(D_2O) plus that predicted by a model for hydration water will slightly reduce the scattered intensity found for H_2O in the corresponding fit below its true value. But the modification of its shape can be neglected.

(iii) It is assumed that the small difference in the water dynamics caused by the mass difference of the isotopes H and D has a negligible effect on the dynamics of PM, so that for our purpose the latter can be considered as approximately identical in the two samples, PM(H_2O) and PM(D_2O). This assumption may be justified as follows: Differences in the dynamics between H_2O hydrated and D_2O hydrated PM are mainly due to an isotope effect in the coupling of water molecules to the PM motions. This coupling is mainly effective in energy ranges where an appreciable overlap exists between the densities of state of water and purple membrane. Furthermore for the present purpose this overlap is only relevant in the low-energy regime, where diffusive motions of H_2O molecules are observed, since we are not studying intramolecular vibrations in this work. As we will see later (see sections 4 and 5), the part of the PM dynamics we are concerned with here corresponds to local diffusive motions which energetically coincide roughly with the spectrum due to translational diffusion within the hydration water layers. We expect that, similar to the case of bulk water at room temperature, the diffusion coefficients of H_2O and D_2O within the hydration layers differ by less than 10%. We may assume that this difference will be only partially transmitted via the coupling phenomenon to PM, so that the part of PM dynamics which is of interest in our context should be identical within a few percent in the two different samples under study. Therefore we are convinced that this isotope effect can be neglected in the above sense. The fitting procedure employed in the comparison of different measured spectra, and especially for the detection of small spectral differences, requires a precise knowledge of the spectrometer energy resolution function. We have converted the measured vanadium spectra into analytical functions by fitting a sum of Lorentzian functions to them. Because of the intrinsically close-to-Lorentzian shape of crystal reflections in backscattering geometry, and because most of the dynamical models for diffusive motions, which we wish to apply lead to scattering functions consisting of sums or series of Lorentzians, this choice suggests itself. Excellent fits were obtained with a sum of five Lorentzians with widths, positions and weight factors as free parameters. This can be appreciated in figs. 2a and 2b, showing the results for the scattering angle $\phi = 90.4°$ and the orientation angles $\alpha = 45°$ and $\alpha = 135°$, respectively, of the vanadium plate relative to the incident beam.

4. The fitting procedure

The following general expression [10] was used to represent the resolution-broadened, measured

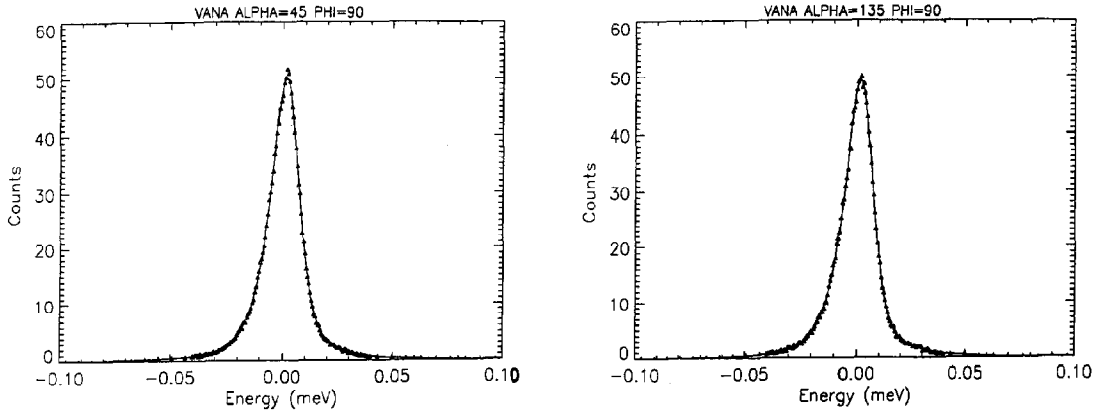

Fig. 2. Vanadium spectra at scattering angle $\phi = 90.4°$, for two different sample orientations α, fitted with a sum of five Lorentzians. triangles: experimental points, solid line: fit. (a) $\alpha = 45°$; (b) $\alpha = 135°$.

scattering functions:

$$S_{meas}(Q, \omega) = F_N \exp(-\hbar\omega/2k_BT) \times S_{res}(Q, \omega) \otimes S_{theor}(Q, \omega). \quad (1)$$

F_N = normalisation factor; $\exp(-\hbar\omega/2k_BT)$ = detailed balance factor; $S_{res}(Q, \omega)$ = resolution function represented by a sum of Lorentzians, as described above; $\otimes$ = convolution operator; $S_{theor}(Q, \omega)$ = model of the incoherent scattering function. The phenomenological expression, used in the fit of $PM(D_2O)$ data, reads

$$S^{PM}_{theor}(Q, \omega) = A_{PM}\delta(\omega) + (1 - A_{PM})L(H_{PM}, \omega) + B_{PM}, \quad (2)$$

where A_{PM} = Q-dependent weight of measured elastic component; $L(H_{PM}, \omega)$ = quasielastic Lorentzian-shaped component with width (HWHM) equal to H_{PM}; B_{PM} = linear "background", mainly due to acoustic phonon-like excitations. Apart from the trivial normalisation factor F_N, there are four free parameters in this fit: A_{PM}, H_{PM} and the constant and slope of B_{PM}. Figs. 3a and 3b show the results obtained at the scattering angle $\phi = 90.4°$ for the two sample orientations $\alpha = 45°$ and $\alpha = 135°$. It is obvious from the quality of these fits that the simple phenomenological model employed is entirely sufficient for the present purpose. In table 1 the numerical values of the parameters A_{PM} and H_{PM} are listed. Qualitatively it can be said that the quasielastic linewidths are of the order of 10 μeV (HWHM) for both sample orientations, but larger by an average factor of about 1.4 for $\alpha = 45°$. This feature will be discussed in more detail in a later publication. The behaviour of B_{PM} will not be discussed further, since it is determined by the scattering intensity far away from the quasielastic peak region and thus completely model-independent. For the fit of the $PM(H_2O)$ spectra a "H_2O" model was added to $S_{theor}(Q, \omega)$ to give:

$$S_{theor}(Q, \omega) = S^{PM}_{theor}(Q, \omega) + S^{H_2O}_{theor}(Q, \omega), \quad (3)$$

where we started from the expression:

$$S^{H_2O}_{theor}(Q, \omega) = C\left(j_0^2(Qr)\delta(\omega) + \sum_{n=1}^{\infty}(2n+1) \times j_n^2(Qr)S_n(\omega)\right) \otimes S_{TD}(Q, \omega) + B_{H_2O}. \quad (4)$$

Apart from the "concentration" factor C, this is the rotational diffusion model [11], which approximates the local motion by diffusion on a spherical surface with the radius r. It is folded with a single Lorentzian $S_{TD}(Q, \omega)$ for translational diffusion; j_n are the spherical Bessel functions, C is

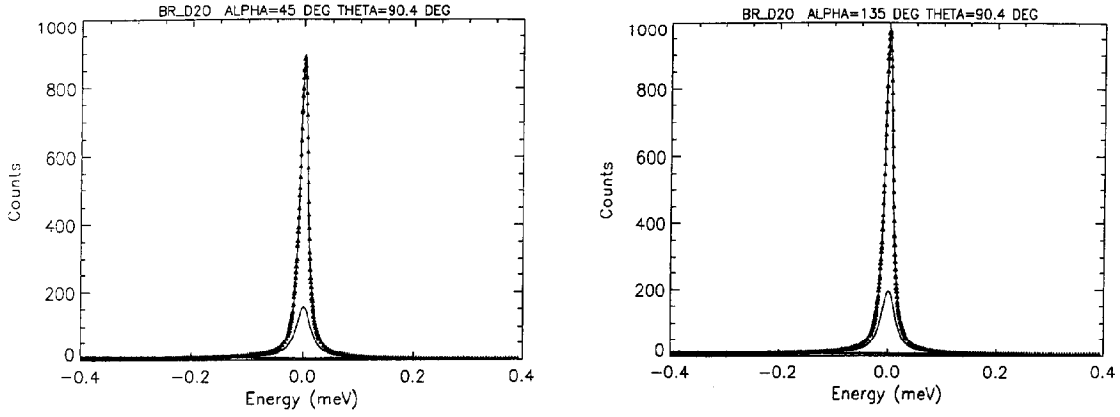

Fig. 3. $PM(D_2O)$ spectra at scattering angle $\phi = 90.4°$; triangles: experimental points; solid lines (result of the fitting procedure, from top to bottom): complete scattering function, fitting the measured spectra; quasielastic component due to local diffusive proton motion; linear "background". The first two curves also include the linear "background". (a) $\alpha = 45°$; (b) $\alpha = 135°$.

defined relative to the concentration of PM in the system PM(H_2O), which is set equal to 1. The energy-dependent factors $S_n(\omega)$ are Lorentzians with HWHM = $n(n+1)D_r$, where D_r is the rotational diffusion constant. As a further simplifying approximation we have retained only the first Lorentzian, $S_1(\omega)$, in this series, since higher terms become important only at larger Q. For this purpose $S_n(\omega)$ in eq. (4) was replaced by $S_1(\omega)$, allowing the replacement of the structure factor sum $\Sigma_{n=1}^{\infty}(2n+1)j_n^2$ (Qr) by $[1-j_0^2(Qr)]$ and thus conserving the energy integral of $S_{\text{theor}}^{H_2O}(Q, \omega)$. The radius r was set equal to 0.98 Å, which is close to the O–H distance of the H_2O molecule. This value has also been used in a successful description of the local diffusive proton motion in bulk water [12]. The additional free parameters in the fit procedure are therefore C, D_r and the quasielastic linewidth H_{TD} of the translational diffusion Lorentzian. This simple model must certainly be considered as a crude approximation of reality; but it allows a relatively precise determination of the volume available for the fast diffusive local proton motion and of the corresponding local diffusion rate. As in the case of the PM(D_2O) spectra, the nonlinear least-squares fitting calculations were carried out on each spectrum individually (see figs. 4a and 4b, as an example for scattering angle $\phi = 90.4°$). This allows us, as a cross-check of the fit results, to verify whether the constant model parameters C and D_r are actually found to be Q independent. This is indeed so: for the "concentration" factor we obtain $C = 0.55 \pm 0.07$, and for the linewidth (HWHM) of the rotational component we find $H_r = 2D_r = 66.4 \pm 10.4$ μeV. This should be compared to the linewidths H_{PM} and H_{TD} which are smaller by roughly an order of magnitude (see table 1). In fact, if the H_r values are averaged separately for $\alpha = 45°$ and $\alpha = 135°$, there is a tendency to slightly smaller values (by 5%) of H_r at $\alpha = 45°$, suggesting that the local diffusive proton motion is not completely isotropic. It is interesting to note that these rotational diffusion rates are about six times smaller than those observed in bulk water at room temperature [12].

The line-widths H_{TD} of the TD Lorentzian, resulting from the fits are plotted as a function of Q^2 in fig. 5. They turn out to be significantly larger in the case of $\alpha = 135°$ (full circles) as compared to $\alpha = 45°$ (open circles).

5. Long-range translational diffusion

From the observed orientation dependence it is clear that the motion described by the TD Lorentzian is strongly anisotropic. The TD linewidths, H_{TD}, observed for $\alpha = 135°$ are significantly larger than those observed for $\alpha = 45°$. In

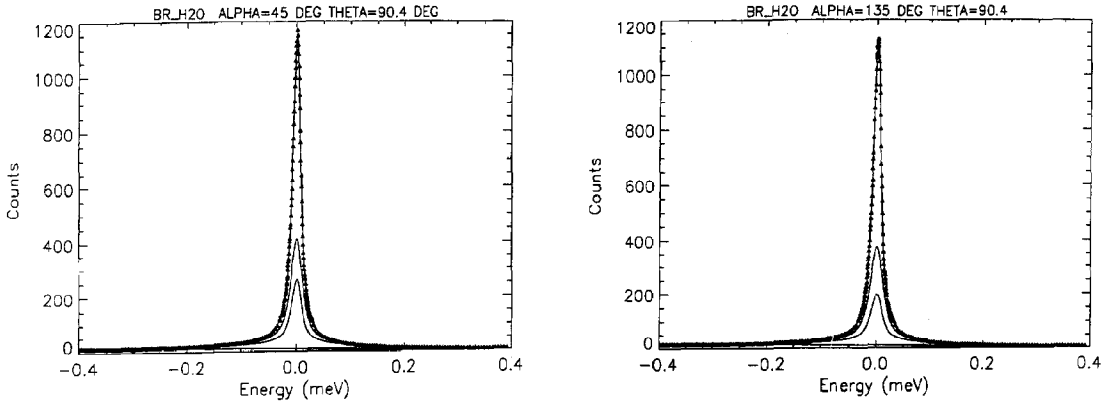

Fig. 4. PM(H_2O) spectra at scattering angle $\phi = 90.4°$; triangles: experimental points, solid lines (results of the fitting procedure, from top to bottom): complete scattering function; sum of quasielastic scattering from PM and H_2O; H_2O component of the scattering function; linear "background". The first three curves also include the linear "background" (a) $\alpha = 45°$; (b) $\alpha = 135°$.

Table 1

Numerical values of the parameters H_{PM}, H_{TD}, H_r and A_{PM} as obtained from the fit of the theory to the spectra measured at 11 different scattering angles ϕ and two sample orientations: upper part $\alpha = 45°$, lower part $\alpha = 135°$. H_{PM}, H_{TD} and H_r are the quasielastic linewidths (HWHM) for local proton motion in PM, translational and rotational proton diffusion in the hydration water, respectively; A_{PM} is the phenomenological EISF of PM; for details see the text

NR.	ϕ (deg)	H_{PM} (μeV)	H_{TD} (μeV)	H_r (μeV)	A_{PM}
$\alpha = 45°$					
1	24.20	11.81	3.79	50.59	0.926
2	35.45				
3	48.12				
4	62.16	8.93	5.60	67.69	0.723
5	76.30	12.79	5.17	73.53	0.739
6	90.38	9.45	4.44	76.05	0.679
7	103.05	11.25	3.62	73.15	0.663
8	115.70	13.14	3.06	69.81	0.655
9	128.40	14.62	1.76	58.31	0.653
10	141.08	13.76	1.24	55.66	0.631
11	155.16	14.40	0.87	56.68	0.612
$\alpha = 135°$					
1	24.20	4.53	5.44	69.83	0.840
2	35.45	3.57	6.68	67.05	0.746
3	48.12	4.44	8.40	71.36	0.698
4	62.16	7.52	8.74	79.06	0.720
5	76.30	8.59	8.38	81.35	0.680
6	90.38	9.01	6.19	74.58	0.651
7	103.05	12.23	5.48	70.52	0.668
8	115.70	13.48	6.06	65.13	0.702
9	128.40				
10	141.08				
11	155.16	15.90	0.24	36.82	0.634

addition to this we note, that the smaller, but finite, values of H_{TD} observed for $\alpha = 45°$ are probably increased due to MSC combinations of scattering from proton motions parallel to the plane with that due to proton motions perpendicular to it. Thus the true anisotropy is presumably stronger than observed. The decrease of H_{TD}, as $Q = 0$ is approached, suggests that we have indeed observed translational diffusion. We have in fact succeeded in confirming this result very recently by pulsed-field gradient (PFG)-NMR spin-echo measurements on a PM(H_2O) sample at the same level of hydration, yielding a proton self-diffusion coefficient D_s of 4.4×10^{-6} cm^2 s^{-1} [13].

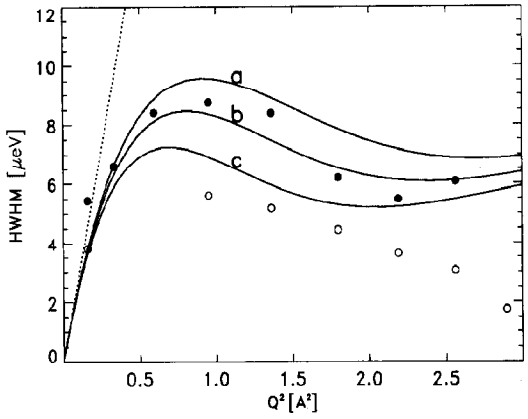

Fig. 5. The Q-dependent linewidths, H_{TD}, of quasielastic scattering due to long-range translational diffusion of hydration water; dotted line: DQ^2 behaviour of the linewidth in the small-Q limit, corresponding to a diffusion coefficient $D_s = 4.4 \times 10^{-6}$ cm^2 s^{-1}; solid circles: values obtained from the fit to the ($\alpha = 135°$) spectra; open circles: values from the fit to the ($\alpha = 45°$) spectra (see table 1); solid lines: linewidths calculated from a jump diffusion model with different jump distances d: (a) $d = 4.7$ Å; (b) $d = 5.0$ Å; (c) $d = 5.4$ Å.

It is well known that in the limit of small Q the TD linewidth is equal to $D\,Q^2$. The corresponding straight line is shown in fig. 5, and it is seen, that this is consistent with our data. However, since these are not yet corrected for MSC, we can only expect a qualitative agreement at present. A more precise analysis including MSC corrections will be published soon [13]. At the present stage we will limit the discussion of H_{TD} to the comparison with a rather simple isotropic jump diffusion model, which is however capable of predicting qualitatively the deviation of the Q dependence of H_{TD} from the DQ^2 behaviour, when Q is not small compared to the reciprocal jump distance. The jump-diffusion model, in its simplest form, describes a random walk of the diffusing particle on a Bravais lattice of sites available for diffusion [14]. For a single-crystal its incoherent scattering function is given by the simple Lorentzian,

$$S_{TD}(Q, \omega) = \frac{f(Q)/\tau}{[f(Q)/\tau]^2 + \omega^2} \frac{1}{\pi}. \qquad (5)$$

In the case of a polycrystalline sample the angular average of eq. (5) is required. In order to avoid the corresponding numerical integration, one may approximate the average by calculating the orientational mean of the width function, $H_{TD} = \langle f(Q)/\tau \rangle_\Omega$. This is equal to

$$H_{TD} = \frac{1 - \sin(Qd)/Qd}{\tau}, \qquad (6)$$

where d is the distance between nearest-neighbour diffusion sites. Given the apparent anisotropy of the diffusion process in the purple membrane, the angular average of $f(Q)$ in our case has to be performed over all directions of the proton displacement within the PM plane, and not over the whole solid angle 4π. Unfortunately this again requires numerical integration. To avoid this we have proceeded in the following way, in order to obtain an approximate interpretation of the measured H_{TD} values:

(1) H_{TD}, measured at $\alpha = 135°$, was compared to expression (6), calculated for several different values of the jump distance d. For $d = 5$ Å we obtain reasonable agreement (curve b in fig. 5). The Q-dependent shape of the H_{TD} curve is rather sensitive to small changes in d. This is demonstrated in fig. 5 for $d = 4.7$ Å (curve a) and $d = 5.4$ Å (curve c).

(2) The jump distance d, determined using a model for three-dimensional diffusion, must be interpreted in a different way, if the diffusion process is restricted to two dimensions. In fact, when a diffusion constant D_s is determined, this is (independently of the dimensionality of the motion) directly related to the mean square displacement $\langle d_Q^2 \rangle$ in the direction of Q, by the relation $D_s = \langle d_Q^2 \rangle / 2\tau$, where τ is the observation time. For instance, if τ is the mean residence time of the diffusing particle on a diffusion site, we have $\langle d_Q^2 \rangle = \frac{1}{3}d^2$ for three-dimensional diffusion, but $\langle d_Q^2 \rangle = \frac{1}{2}d^2$ for diffusion in a plane. Thus we can calculate the average jump distance in the membrane plane from the above three-dimensional value (5 Å), using the relation

$$\tfrac{1}{2}(d_{2D})^2 = \tfrac{1}{3}(d_{3D})^2. \qquad (7)$$

One obtains $d_{2D} = 4$ Å.

6. Discussion and conclusion

We have reported the results of high-resolution QINS experiments on purple membrane, hydrated at 100% relative humidity. The present analysis concerned specifically the dynamics of the hydration layers, which we have separated from the dynamics of the membrane itself by careful comparison of purple membrane spectra obtained for samples hydrated in H_2O and in D_2O, respectively. We were able to show that the protons are participating in a two-dimensional long-range translational diffusion process parallel to the membrane plane (presumably mainly of water molecules), which is about five times slower than that known for bulk water. This is accompanied by a local (rotational) motion of molecules, six times slower than in bulk water. On the other hand a translational jump distance of about 4 Å was obtained, three times larger than that of bulk water at room temperature [12]. We believe that these results are related and consistent with each other. Translational and rotational diffusion may be expected to be relatively slow because of spatial restrictions. These are obviously strong perpendicular to the membrane plane. But even parallel to the plane the space available for diffusive motion is somewhat less open than in bulk water, due to a certain ruggedness of the membrane surface. This is caused by the geometrical arrangement of the BR polypeptide chain, consisting of seven helical sections, well embedded within the membrane, but linked by loops protruding out of the membrane surface. The diffusion jump length is an average distance between neighbouring potential minima of the diffusing particle. Therefore this length can be considered to some extent to be a measure of the mean spatial extension of barriers or obstacles to the motion. Neighbouring water molecules may alternate with protruding loops or other molecular subunits at the membrane surface as obstacles, which easily makes the relatively large jump distance observed plausible.

It is clear that our analysis is based on a number of approximations and simplifying assumptions as described in sections 3 to 5. We intend to improve some of this in the near future.

In particular we expect to obtain more quantitative results after having carried out MSC corrections. Preliminary MSC calculations, performed to estimate the relative importance of these effects, have shown that such corrections will not change our qualitative conclusions.

Acknowledgement

We thank the staff of the Rutherford–Appleton Laboratory for the competent assistance during the QINS experiments, especially Mr. M. Adams, Dr. C.J. Carlile and the Sample Environment team.

References

1 R. Henderson and P.N.T. Unwin, Nature 257 (1975) 28.
2 R. Henderson, J.M. Baldwin, T.A. Ceska, F. Zemlin, E. Beckmann and K.H. Downing, J. Mol. Biol. 213 (1990) 899.
3 M.H.J. Koch, N.A. Dencher, D. Oesterhelt, H.-J. Plöhn, G. Rapp and G. Büldt, EMBO J. 10 (1991) 521.
4 D. Oesterhelt and W. Stoeckenius, Proc. Natl. Acad. Sci. USA 70 (1973) 2853.
5 N.A. Dencher, Endocyt. C. Res. 5 (1988) 1.
6 N.A. Dencher, G. Büldt, J. Heberle, H.-D. Höltje and M. Höltje, in: NATO ASI Series B Vol. 291, "Proton Transfer in Hydrogen-Bonded Systems", ed. T. Bountis (Plenum Press, New York, 1992) p. 171.
7 R.E. Lechner, N.A. Dencher, J. Fitter and G. Büldt, Physica Scripta, T45 (1992) 236.
8 C.J. Carlile and M.A. Adams, Physica B 182 (1992) 431.
9 R.E. Lechner, G. Badurek, A.J. Dianoux, H. Hervet and F. Violino, J. Chem. Phys. 73 (1980) 934.
10 R.E. Lechner and C. Riekel, in: Springer Tracts in Modern Physics, Vol. 101. Neutron scattering and muon spin rotation, ed. G. Höhler, (Springer, Berlin, 1983) p. 1.
11 V.F. Sears, Can. J. Phys. 45 (1967) 237.
12 J. Teixera, M.-C. Bellissent-Funel, S.H. Chen and A.J. Dianoux, Phys. Rev. A 31 (1985) 1913.
13 R.E. Lechner, J. Fitter, Th. Dippel and N.A. Dencher, Solid State Ionics, to be published.
14 C.T. Chudley and R.J. Elliott, Proc. Phys. Soc. (London) 77 (1961) 353.